Published in final edited form as:
Langmuir. 2008 September 16; 24(18): 10524–10531. doi:10.1021/la801762h.

DNA Curtains and Nanoscale Curtain Rods: High-Throughput Tools for Single Molecule Imaging

Teresa Fazio[†,§], **Mari-Liis Visnapuu**[‡,§], **Shalom Wind**[†], and **Eric C. Greene**[*,‡]
Department of Applied Physics and Applied Mathematics, Center for Electron Transport in Molecular Nanostructures, NanoMedicine Center for Mechanical Biology, Columbia University, 020 Schapiro CEPSR, 530 West 120th Street, New York, New York 10027, and Department of Biochemistry and Molecular Biophysics, Columbia University, 650 West 168th Street, Black Building Room 536, New York, New York 10032

Abstract

Single molecule visualization of protein–DNA complexes can reveal details of reaction mechanisms and macromolecular dynamics inaccessible to traditional biochemical assays. However, these techniques are often limited by the inherent difficulty of collecting statistically relevant information from experiments explicitly designed to look at single events. New approaches that increase throughput capacity of single molecule methods have the potential for making these techniques more readily applicable to a variety of biological questions involving different types of DNA transactions. Here we show that nanofabricated chromium barriers, which are located at strategic positions on a fused silica slide otherwise coated with a supported lipid bilayer, can be used to organize DNA molecules into molecular curtains. The DNA that makes up the curtains is visualized by total internal reflection fluorescence microscopy (TIRFM) allowing simultaneous imaging of hundreds or thousands of aligned molecules. These DNA curtains present a robust experimental platform portending massively parallel data acquisition of individual protein–DNA interactions in real time.

Introduction

Single molecule techniques have revealed insights into previously inaccessible aspects of biology,[1–3] and this field is now poised to profoundly impact the way that biological macromolecules can be studied. However, meeting the oncoming challenges will require the development of more robust, user-friendly, high-throughput experimental platforms that can be readily applied to a broad range of biochemical systems.

Many single molecule techniques require that the macromolecules under investigation be anchored to a solid surface. It is essential to minimize nonspecific interactions with the surface that may perturb their biological properties. Traditional approaches for passivating surfaces have included nonspecific blocking agents (e.g., BSA or casein) or covalent modification with polyethylene glycol (PEG).[4,5] Nonspecific blocking proteins often do not work well enough to prevent surface adsorption of other molecules.[6] PEGylated surfaces are efficient at preventing nonspecific interactions between proteins or nucleic acids and the underlying surface, but PEG alone may not be sufficient in all cases. More recently, vesicle

[*]To whom correspondence should be addressed. ecg2108@columbia.edu.
[†]Department of Applied Physics and Applied Mathematics, Center for Electron Transport in Molecular Nanostructures, NanoMedicine Center for Mechanical Biology.
[‡]Department of Biochemistry and Molecular Biophysics.
[§]These authors contributed equally.

encapsulated reactions have been used in single molecule analysis.[7,8] Vesicle encapsulation is a promising approach that makes use of the native environment provided by lipid membranes, but has limited potential for experiments involving macromolecules that can not be confined within vesicles or those requiring successive addition of high-molecular weight components.

Single molecule techniques are also impeded by the difficulty of collecting statistically relevant information. This can be problematic when the reactions under investigation require the use of long DNA substrates, especially when the reactions themselves are inefficient and/or involve rare intermediates. Procedures for anchoring numerous, long DNA molecules to surfaces are present in the literature, and each has potential for specific situations, but they also suffer drawbacks for biochemical applications. For example Bensimon et al., developed "DNA combing",[9] which has evolved into a powerful tool.[10] Combed DNA is anchored to a hydrophobic glass slide, and aligned with a receding air–water meniscus, yielding molecules adhered to the glass by multiple contact points and stretched beyond the length of normal B-DNA. The hydrophobic surfaces required for combing and the resulting distortion of the DNA may not be compatible with many proteins. In addition, while the combed DNA molecules are aligned along a common direction their ends are not aligned relative to one another nor is the orientation of the DNA defined with respect to its sequence. In another elegant approach, Kabata and colleagues reported that "belts" of λ-DNA could be stretched between two aluminum electrodes, which they used to visualize the motion of RNAP and *Eco*RI by fluorescence microscopy.[11,12] However broader use of this technique has not been realized.[13] Recently, Guan and Lee have demonstrated that highly ordered arrays of DNA molecules can be stamped onto PDMS (polydimethyl siloxane) with a method based on molecular combing.[14] This technology is promising, but protein adsorption to unmodified PDMS may present a limitation for biochemical applications. Prentiss and colleagues have used an approach in which magnetic beads were linked to the free ends of DNA molecules anchored to a glass surface.[15] Kim et al., reported a similar approach, in which they anchored molecules of λ-DNA to a PEGylated surface and stretched the DNA with buffer flow.[16] In each of these examples they concurrently detect ~100–200 molecules, but required 10× magnification to expand the field-of-view, thus the overall density of the anchored DNA remained quite low.[16] Finally, Schwartz and co-workers have pioneered single DNA molecule optical mapping techniques,[17,18] but these approaches may not be applicable for real time biochemical analysis of protein–DNA interactions.

To address these challenges we have developed "DNA curtains", which allow simultaneous imaging of on the order of one hundred individual DNA molecules.[19] Curtains are assembled by anchoring one end of a biotinylated DNA molecule to a lipid bilayer, which provides an inert environment compatible with a wide range of biological molecules.[20] The bilayer also permits long-range two-dimensional motion of the lipid-tethered DNA molecules. We have taken advantage of this mobility by using hydrodynamic force to organize the DNA molecules at microscale diffusion barriers, which are manually etched into the surface of the flowcell and oriented perpendicular to the direction of buffer flow. Lipids within the bilayer can not traverse the etched barrier,[21] therefore the lipid-tethered DNA molecules accumulate along the leading edges of these barriers.[19] However, the etched barriers are difficult to control and also compromise the quality of the optical surface, leading to problems such as light scattering, uneven alignment of DNA, nonspecific protein adsorption, inefficient coverage of the viewing area, and a high failure rate.

In this work, we use electron-beam lithography to engineer chromium barriers with nanometer (nm) scale features and use these nanoscale barriers to assemble curtains of DNA. The shape of the barriers and the fluidity of the bilayer are used to organize the DNA into patterns in which all of the molecules are aligned with respect to one another. These

barriers are simple and robust, they do not interfere with optical imaging of the fluorescent DNA molecules, and they can be precisely constructed on the surface of a microfluidic sample chamber. Using these nanoscale barriers we can concurrently image several hundred and even several thousand aligned DNA molecules in a single field-of-view. These DNA curtains provide a powerful experimental platform enabling rapid data acquisition from thousands of individual molecules and offer a myriad of potential applications.

Materials and Methods

Barrier Construction by E-beam Lithography

Fused silica slides were cleaned in NanoStrip solution (CyanTek Corp.) for 20 min, then rinsed with acetone and isopropanol and dried with N_2. The slides were spin-coated with a double layer of polymethyl-methacrylate (PMMA), first using molecular weight 25K plus 3% anisole, and then using 495K plus 1.5% in anisole (MicroChem). This was followed by a layer of Aquasave conducting polymer (Mitsubishi Rayon). Each layer was spun at 4000 rpm for 45 s using a ramp rate of 300 rpm/s. Patterns were written by E-beam lithography using an FEI Sirion scanning electron microscope equipped with a pattern generator and lithography control system (J. C. Nabity, Inc.). After the pattern was written the Aquasave was washed off with deionized water and the sample dried with N_2. Resist was developed using a 3:1 solution of isopropanol to methyl isobutyl ketone (MIBK) for 1 min with ultrasonic agitation at 5 °C. The substrate was then rinsed in isopropanol and dried with N_2. A thin layer of chromium was deposited using a Semicore electron beam evaporator. For this work, Cr films of ~20–40 nm were used. To effect lift-off, the coated substrate was submerged in a 65 °C acetone bath for 30 min, and then gently sonicated. Following lift-off, samples were rinsed with acetone to remove stray chromium flakes and dried with N_2. Barriers were imaged using a Hitachi 4700 scanning electron microscope and a PSIA XE-100 Scanning Probe Microscope in noncontact mode. Optical images of the barriers were taken with a Nikon Eclipse ME600 at either 10× or 20× magnification (as indicated).

Lipid Bilayers and DNA Curtains

Flowcells and DNA curtains were constructed as previously described.[19] All lipids were purchased from Avanti Polar Lipids and liposomes were prepared as previously described. In brief, a mixture of DOPC (1,2-dioleoyl-*sn*-glycero-phosphocholine), 0.5% biotinylated-DPPE (1,2-dipalmitoyl-*sn*-glycero-3-phosphoethanolamine-*N*-(cap biotinyl)), and 8% mPEG 550-DOPE (1,2-dioleoyl-*sn*-glycero-3-phosphoethanolamine-*N*-[methoxy(polyethylene glycol)-550]). The mPEG 550-DOPE is not essential for assembly of the DNA curtains, but rather helps minimize nonspecific binding of quantum dot tagged proteins to the lipid bilayer. Liposomes were applied to the sample chamber for 30 min. Excess liposomes were flushed away with buffer containing 10 mM Tris-HCl (pH 7.8) and 100 mM NaCl. The flowcell was then rinsed with buffer A (40 mM Tris-HCl (pH 7.8), 1 mM DTT, 1 mM $MgCl_2$, and 0.2 mg/ml BSA) and incubated for 15 min. Neutravidin (660 nM) in buffer A was then injected into the sample chamber and incubated for 10 min. After rinsing with additional buffer A, biotinylated λ-DNA (~10 pM; 48.5 kb) prestained with YOYO1 (1 dye per 600 base pairs) was injected into the sample chamber, incubated 10 min, and unbound DNA was removed by flushing with buffer at 0.1 mL/min. For imaging, the buffers also contained 100 pM YOYO1 along with an oxygen scavenging system comprised of 1% (w/v) glucose, 60 mM β-mercaptoethanol, glucose oxidase (100 units/mL) and catalase (1,560 units/mL). Application of flow caused the DNA molecules to align along the leading edges of the diffusion barriers. The flow was stopped for 5 min allowing the DNA to diffuse toward the center of the barriers. The flow was started at 0.1 mL/min for 30 s and the flow on–off cycle was repeated 3–5 times until DNA curtains of even density formed along the diffusion barriers.

TIRFM

The basic design of the microscope used in this study has been previously described.[22] The beam intensity at the face of the prism was typically ~10–15 mW. Images were detected with a back-illuminated EMCCD detector (Photometrics, Cascade 512B). TIRFM images were collected using a 60x water immersion objective lens (Nikon, 1.2 NA, Plan Apo) or a 10× objective (Nikon, 0.45 NA, Plan Apo), as indicated.

Restriction Enzymes and Msh2-Msh3

For complete digests, 700 μL of the desired restriction enzyme in reaction buffer A (40 mM Tris-HCl (pH 7.8), 1 mM $MgCl_2$, 1 mM DTT, and 0.2 mg/ml BSA) plus 50 mM NaCl and 10 mM $MgCl_2$ was injected at 0.2 mL/min. All restriction enzymes were purchased from NEB and the amounts of enzymes used were as follows: NheI (100 units/ml); XhoI (100 units/ml); *Eco*RI (100 units/ml); NcoI (50 units/ml); PvuI (50 units/ml); and SphI (50 units/ml). Images of the DNA molecules were collected before the restriction enzyme injection and after all of the enzyme solution had flown through. For partial digests, the amount of *Eco*RI was reduced to 20 units/ml and 700 μL was injected at 0.4 mL/min.

Msh2-Msh3 was purified as described,[23] and TIRFM experiments with Msh2-Msh3 were performed essentially as described for our previously published experiments with Msh2-Msh6.[24] In brief, HA-tagged Msh2-Msh3 was incubated with anti-HA antibody conjugated quantum dots at 1:2 protein:quantum dot ratio for 15 min in Buffer A plus 50 mM NaCl. 50 μL of 1.5 nM quantum dot tagged Msh2-Msh3 was then injected at 0.1 mL/min to allow efficient binding. The flow rate was increased to 0.4 mL/min for data collection, and the binding distributions were quantitated as described.[25]

Results

Nanoscale Barriers to Lipid Diffusion

The use of barriers to corral lipids within supported bilayers has been pioneered by Boxer and colleagues.[26] Inspired by these studies, we demonstrated that mechanical barriers to lipid diffusion can also be used to organize DNA molecules into curtains at defined locations on a fused silica surface.[19] We have shown that these curtains serve as an effective platform for the study of protein–DNA interactions at the single molecule level.[24,25,27] The principles behind this approach are outlined in Figure 1. To make the curtains, DNA is first anchored by one end to a supported lipid bilayer coating the surface of the sample chamber (Figure 1B and C). In the absence of a hydrodynamic force the molecules are randomly distributed on the surface, but lie outside of the detection volume defined by the penetration depth of the evanescent field (~150–200 nm).[28] Application of flow pushes the DNA through the sample chamber with one end anchored to the bilayer. The barriers are oriented perpendicular to the direction of flow at strategic locations in the path of the DNA (Figure 1B and C); this halts the movement of the molecules causing them to accumulate and extend parallel to the surface.[19]

Previously we used micrometer-scale diffusion barriers prepared by manually scoring the surface with a diamond-tipped scribe.[19,22,24,25,27] Manual etching is simple, yet inherently difficult to control and, as indicated above, can cause several problems with data acquisition. As an alternative we sought to apply lithographic techniques for generating precisely patterned nanoscale barriers that could be used to organize DNA molecules into curtains, making the most efficient use of available surface area. Figure 2A shows a cartoon representation of a desired surface pattern comprised of an interlocking series of bracket-shaped barriers, and the important features of the design are indicated. Guide channels ensure efficient capture of approaching DNA molecules tethered to the bilayer.

Perpendicular barriers form the “curtain rods” against which the DNA molecules are aligned. The parallel barriers of the guide channels also prevent the molecules from sliding off the edges of the perpendicular barriers when buffer flow is transiently paused (see below).

An optical image of a chromium barrier pattern prepared by direct-write electron beam (E-beam) lithography is shown in Figure 2B. Fluorescence images of the same type of barrier collected at 60x magnification after deposition of a supported bilayer containing fluorescent lipids (0.5% rhodamine-DHPE), confirm that the barriers do not prevent bilayer deposition (Figure 2C). The image in Figure 2D shows a section of fused silica surface with a 2 × 3 series of chromium barrier sets. Figure 2E shows an atomic force microscopy (AFM) image illustrating a representative single barrier that is 31 nm tall (data not shown). The height of the barriers can be accurately controlled as required for specific experimental needs. We have successfully tested barrier heights ranging from ~20 to 200 nm, and we believe that barriers only a few nm in height would also be suffice.[26] Figure 2F shows a scanning electron microscopy (SEM) image of a parallel chromium barrier revealing a width 100 nm. In contrast to the uniform chromium barriers, the width of the etched barriers is typically ~5–10 μm and they have irregular topology (not shown).

Assembly of DNA Curtains at Nanoscale Curtain Rods

To assemble curtains, biotinylated λ-DNA is tethered to the bilayer through tetravalent neutravidin that is in turn attached to a subset of lipids that have biotinylated head groups. The DNA molecules are pushed in the direction of the diffusion barriers through the application of a flow force. This pushes the DNA into the barrier patterns where they accumulate at the ends of the guide channels. Flow is then briefly terminated, allowing the molecules to diffuse freely within the bilayer. This permits lateral diffusion of the DNA so that they become evenly distributed along the barriers. The DNA is retained within the barrier set because flow is not stopped long enough to allow them to diffuse out of the guide channel openings. Flow can then be resumed, and if necessary this process is repeated at short intervals to achieve even disbursement of the DNA along the barrier edges (see Materials and Methods).

Figure 3A shows an image with λ-DNA organized into curtains within a five-tiered barrier set. There are ~805 individual, molecules of λ-DNA in this field-of-view. When flow is transiently terminated, the DNA molecules diffuse up away from the surface and out of the evanescent field (Figure 3B). This control verified that the DNA molecules are anchored by only one end to the sample chamber surface. Molecules nonspecifically adsorbed to the surface will remain extended when flow is transiently paused and can be excluded from further analysis. When flow is stopped for longer than a few seconds the anchored DNA molecules also begin to move away from the barrier edges, showing that they are not irreversibly anchored to the strips of chromium (Figure 3C). When flow is resumed the DNA molecules are pushed back into the diffusion barriers (Figure 3D).

Figure 3E–G shows a 2 ×3 array of barrier patterns containing λ-DNA viewed at 10× magnification. There are ≥ 1000 DNA molecules per barrier set and 6 sets of barriers, corresponding to ≥6000 individual DNA molecules in this single field-of-view. The amount of DNA applied to the surface, the fraction of biotinylated lipid, the spacing between barrier sets, the number of barriers, and the width of the guide channel openings all dictate the total amount of DNA aligned at any given barrier. Any of these variables can be controlled to adjust the number of DNA molecules as needed.

Orientation Specificity and Optical Restriction Mapping of DNA Curtains

If some fraction of the DNA is bound to the bilayer via its unlabeled end, then this population of DNA will have reversed sequence orientation with respect to those molecules anchored via the biotin tag. Verifying the expected alignment is critical for experiments meant to examine the locations of DNA bound proteins (see below). λ-DNA has five *Eco*RI restriction sites located 21,226 bp, 26,106 bp, 31,747 bp, 39,168 bp and 44,972 bp from the left end of the molecules. If the molecules are in the expected orientation, then complete *Eco*RI digestion of λ-DNA anchored by its left end will yield a tethered fragment of approximately 21 kb, and all of the downstream fragments will be washed from the sample chamber. Similarly, an *Eco*RI digestion of a curtain comprised of λ-DNA biotinylated at the right end should yield much smaller fragments corresponding to a final length of 3.5 kb. Figure 4A–D confirms these predictions, proving that the molecules making up the curtain are tethered in the same orientation.

Optical restriction mapping has evolved into a powerful technique for the physical analysis of large DNA molecules,[17,18,29] and because the DNA curtains are organized with all of the molecules in a defined orientation they provide a simple platform for mapping the locations of specific restriction sites. As shown in Figure 4E, different combinations of restriction sites can be easily mapped within the DNA curtain by successive use of the desired enzymes. In this example, the curtain was sequentially cut with NheI, XhoI, *Eco*RI, NcoI, PvuI, and SphI, and the observed lengths (μm) of the DNA fragments were measured and plotted as a histogram. As shown here, complete restriction digests leave behind tethered DNA fragments whose lengths correspond to the cleavage site closest to the biotinylated ends of the DNA, and any other downstream fragments are washed away. Complete restriction digests can reveal single cleavage sites, and can not map multiple, identical restriction sites throughout the DNA molecules. In contrast, a partial digest should yield a population of discrete fragments whose lengths correspond to each of the restriction sites present in the DNA molecules. To verify this prediction, we performed a partial *Eco*RI digest of curtains made with DNA molecules that were tethered by either the right or the left ends. The lengths of the resulting fragments were then measured and their distributions plotted as histograms (Figure 4F and G). This partial digest strategy was sufficient to identify all five *Eco*RI sites within the phage λ genome. Together these experiments demonstrate that the locations of restriction sites within large molecules can be rapidly identified via optical mapping of the DNA curtains.

The DNA fragment lengths reported above are indicated in microns, and represent an apparent, observed value rather than a direct measure of the actual contour length. To estimate the actual size of any DNA fragment in either microns or base pairs the observed contour length of the DNA in microns must be corrected for the fact that the molecules are not uniformly stretched by the buffer flow and are also not fully extended. The mean extension $\langle x \rangle / L$ of the DNA molecules examined in this study was approximately 0.80, corresponding to ≈0.6 pN of tension. A plot of all the different measured DNA fragment contour lengths in μm versus the known length of fully extended DNA fragments based on their size in either microns or base pairs can be used as a calibration curve to estimate the actual size of the DNA fragments (not shown). Although sufficient for estimating the number of base pairs in relatively large tethered DNA fragments, we note that this empirical relationship breaks down with shorter DNA molecules (≤9kb, not shown), because the tension experienced by the DNA (and therefore the mean extended length) decreases as the molecules get shorter. For example, the SphI ~2.2 kb fragments described above were too short to measure. In addition, smaller DNA fragments tend to diffuse laterally along the barrier edges (data not shown), making it difficult count them directly. As consequence of these two effects, the observed lengths for the shorter fragments are just an approximation and the total number observed was based on the initial number of uncut DNA molecules.

While measurements of these smaller fragment lengths is beyond the scope of this study, it should nevertheless be possible by including a rigorous analysis of signal intensity data and/or accommodating for effects of shear flow on extended polymers, and it may also be possible to restrict their lateral motion with alternative barrier designs.

Visualizing Protein–DNA Interactions with Nanofabricated DNA Curtains

These DNA curtains are useful for analysis of protein–DNA interactions at the level of individual molecules, and are capable of providing statistically relevant information in a single experimental run. To demonstrate this utility we examined the binding distribution of Msh2-Msh3, a protein complex that is involved in postreplicative mismatch repair of small insertion/deletion loops and DNA processing during genetic recombination.[23,30] For this experiment recombinant Msh2-Msh3 bearing an HA epitope tag on Msh2 was labeled with anti-HA tagged quantum dots, as previously described.[24] The tagged proteins were then injected into a sample chamber containing DNA curtains, and the unbound proteins were removed by buffer flow. The DNA molecules and remaining bound proteins were then viewed in the presence and absence of buffer flow (Figure 5A and B). This transient pause in buffer flow is used as a control to verify that the observed proteins are bound only to the DNA and are not bound to the flowcell surface (compare Figure 5, panels A and B). As shown in Figure 5A and C, Msh2-Msh3 bound to the curtains of λ-DNA, but did not display any notably preferred regions or sites, as expected for undamaged, homo-duplex DNA substrates. There are 226 individual DNA molecules and 548 complexes of Msh2-Msh3 in this single field-of-view collected at 60×magnification, highlighting the statistical power of this approach for viewing single protein–DNA complexes.

Discussion

Here we nanofabricate arrays of diffusion barriers, which are used to organize curtains of DNA on a surface coated with a supported lipid bilayer. With these tools we can visualize thousands of individual, perfectly aligned DNA molecules, all arranged in the exact same orientation using TIRFM. These nanofabricated DNA curtains offer numerous advantages that overcome some current limitations of single molecule DNA imaging. The method is simple and robust, the flowcells are reusable, the barriers themselves are highly uniform, and they do not compromise the optical quality of the fused silica or interfere with signal detection. In addition, the bilayer provides an inert environment closely resembling a cell membrane and is compatible with many biological macromolecules, ensuring that the DNA curtains can be used for imaging a range of biochemical systems.[20,26]

Direct-write electron-beam lithography for nanofabricating barrier patterns offers tremendous reproducibility, accuracy, design flexibility, and is particularly advantageous for prototyping devices. The key elements of the barrier design (barrier height, barrier width, shape, etc.) can all be adjusted to accommodate any experimental need with few limitations on the overall pattern other than constraints imposed by the use of lithographic techniques. Moreover, the design flexibility conferred by the use of nanolithography beckons the development of much more complex barrier elements to accommodate and/or manipulate any desired substrate.

Our primary intent was to generate new tools that facilitate massively parallel data collection for single molecule analysis of protein–DNA interactions, yet it is also apparent that the DNA curtains offer a myriad of other potential applications. For example, they enable rapid generation of physical maps of long DNA molecules, and we have demonstrated this with a series of optical mapping assays based on restriction endonuclease cleavage. Because these reactions are performed within a microfluidic sample chamber and DNA is only anchored by

one end, collection of the liberated fragments in sufficient quantities for cloning and further analysis should prove straightforward.

Acknowledgments

We are grateful to Dr. James T. Yardley for valuable advice and discussion throughout this work. We also thank members of our laboratories for insightful discussions and for carefully reading this manuscript. We thank Dr. Jennifer Surtees for providing purified Msh2-Msh3. This research was funded by the Initiatives in Science and Engineering grant (ISE: awarded to E.C.G. and S.W.) program through Columbia University, and by NIH Grant No. GM074739 and an NSF PECASE Award to E.C.G. T.A.F. was supported in part by a National Science Foundation Graduate Research Fellowship. This work was also partially supported by the Nanoscale Science and Engineering Initiative of the National Science Foundation under NSF Award No. CHE-0641523 and by the New York State Office of Science, Technology, and Academic Research (NYSTAR).

References

1. Bustamante C, Bryant Z, Smith SB. Nature 2003;421:423–427. [PubMed: 12540915]
2. Cairns BR. Nat Struct Mol Biol 2007;14:989–996. [PubMed: 17984961]
3. Zlatanova J, van Holde K. Mol Cell 2006;24:317–329. [PubMed: 17081984]
4. Ha T, Rasnik I, Cheng W, Babcock HP, Gauss GH, Lohman TM, Chu S. Nature 2002;419:638–641. [PubMed: 12374984]
5. Heyes CD, Groll J, Möller M, Neienhaus GU. Mol Biosyst 2007;3:419–430. [PubMed: 17533455]
6. Rasnik I, Myong S, Cheng W, Lohman TM, Ha T. J Mol Biol 2004;336:395–408. [PubMed: 14757053]
7. Rhoades E, Gussakovsky E, Haran G. Proc Natl Acad Sci USA 2003;100:3197–3202. [PubMed: 12612345]
8. Cisse I, Okumus B, Joo C, Ha T. Proc Natl Acad Sci USA 2007;104:12646–12650. [PubMed: 17563361]
9. Bensimon A, Simon A, Chiffaudel A, Croquette V, Heslot F, Bensimon D. Science 1994;265:2096–2098. [PubMed: 7522347]
10. Lebofsky R, Bensimon A. Briefings Funct Genom Proteom 2003;1:385–396.
11. Kabata H, Kurosawa O, Arai I, Washizu M, Margarson SA, Glass RE, Shimamoto N. Science 1993;262:1561–1563. [PubMed: 8248804]
12. Kabata H, Okada W, Washizu M. Jpn J Appl Phys 2000;39:7164–7171.
13. Washizu M, Kurosawa O, Arai I, Suzuki S, Shimamoto N. IEEE Trans Ind Appl 1995;31:447–456.
14. Guan J, Lee LJ. Proc Natl Acad Sci USA 2005;102:18321–18325. [PubMed: 16352724]
15. Assi F, Jenks R, Yang J, Love C, Prentiss M. J Appl Phys 2002;92:5584–5586.
16. Kim S, Blainey PC, Schroeder CM, Xie SX. Nat Methods 2007;4:397–399. [PubMed: 17435763]
17. Dimalanta ET, Lim A, Runnheim R, Lamers C, Churas C, Forrest DK, de Pablo JJ, Graham MD, Coppersmith SN, Goldstein S, Schwartz DC. Anal Chem 2004;76:5293–5301. [PubMed: 15362885]
18. Lin J, Qi R, Aston C, Jing J, Anantharaman TS, Mishra B, White O, Daly MJ, Minton KW, Venter JC, Schwartz DC. Science 1999;285:1558–1562. [PubMed: 10477518]
19. Granéli A, Yeykal C, Prasad TK, Greene EC. Langmuir 2006;22:292–299. [PubMed: 16378434]
20. Sackmann E. Science 1996;271:43–48. [PubMed: 8539599]
21. Cremer PS, Boxer SG. J Phys Chem B 1999;103:2554–2559.
22. Granéli A, Yeykal C, Robertson RB, Greene EC. Proc Natl Acad Sci USA 2006;103:1221–1226. [PubMed: 16432240]
23. Surtees JA, Alani E. J Mol Biol 2006;360:523–536. [PubMed: 16781730]
24. Gorman J, Chowdhury A, Surtees JA, Shimada J, Reichman DR, Alani E, Greene EC. Mol Cell 2007;28:359–370. [PubMed: 17996701]
25. Prasad TK, Robertson RB, Visnapuu ML, Chi P, Sung P, Greene EC. J Mol Biol 2007;369:940–953. [PubMed: 17467735]

26. Groves J, Boxer S. Acc Chem Res 2002;35:149–157. [PubMed: 11900518]
27. Prasad TK, Yeykal C, Greene EC. J Mol Biol 2006;363:713–728. [PubMed: 16979659]
28. Axelrod D. Methods Cell Biol 1989;30:245–270. [PubMed: 2648112]
29. Schwartz DC, Li X, Hernandez LI, Ramnarain SP, Huff EJ, Wang YK. Science 1993;262:110–114. [PubMed: 8211116]
30. Langston LD, Symington LS. EMBO J 2005;24:2214–2223. [PubMed: 15920474]

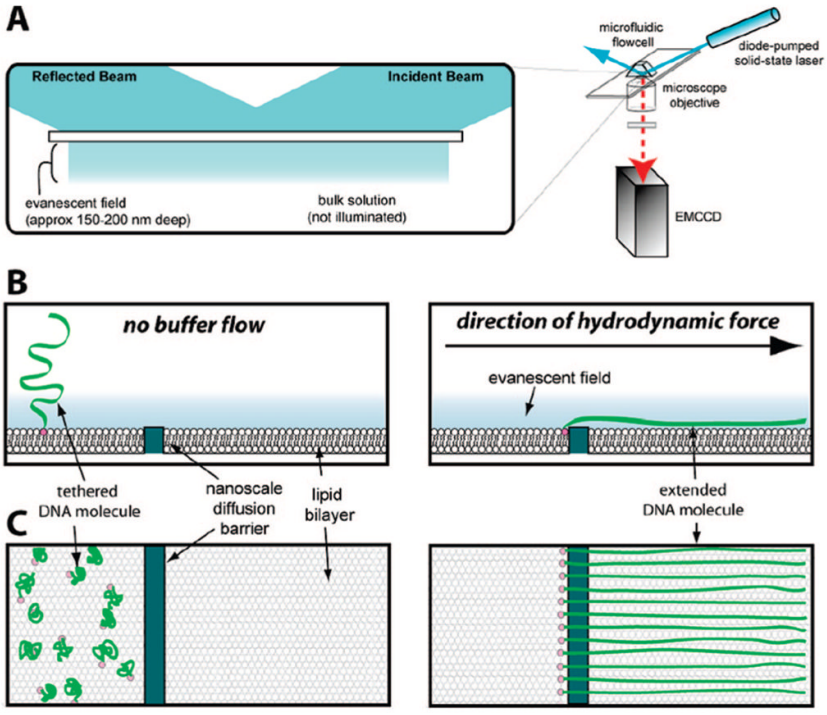

Figure 1.

Conceptual diagram of lipid tethered DNA molecules aligned at a diffusion barrier. Panel (A) shows a diagram of the total internal reflection fluorescence microscope (TIRFM) used to image single molecules of DNA. For imaging by TIRFM the long DNA molecules (48 kb) used in these studies must be extended parallel to the surface of the sample chamber in order to remain confined within the evanescent field. Panels (B) and (C) depict a cartoon illustration of the bilayer on the surface of a fused silica slide along with a barrier and the response of tethered DNA molecules to the application of a hydrodynamic force. The upper and lower panels in (B) and (C) depict views from the side and above, respectively. In the absence of buffer flow (B) the DNA molecules are tethered to the surface, but are not confined within the evanescent field, nor are they aligned at the barrier. As depicted in (C), when flow is applied, the DNA molecules are dragged through the bilayer until they encounter the diffusion barrier, at which point they will align with respect to one another and form a curtain of DNA molecules. Please note that these drawings are not to scale.

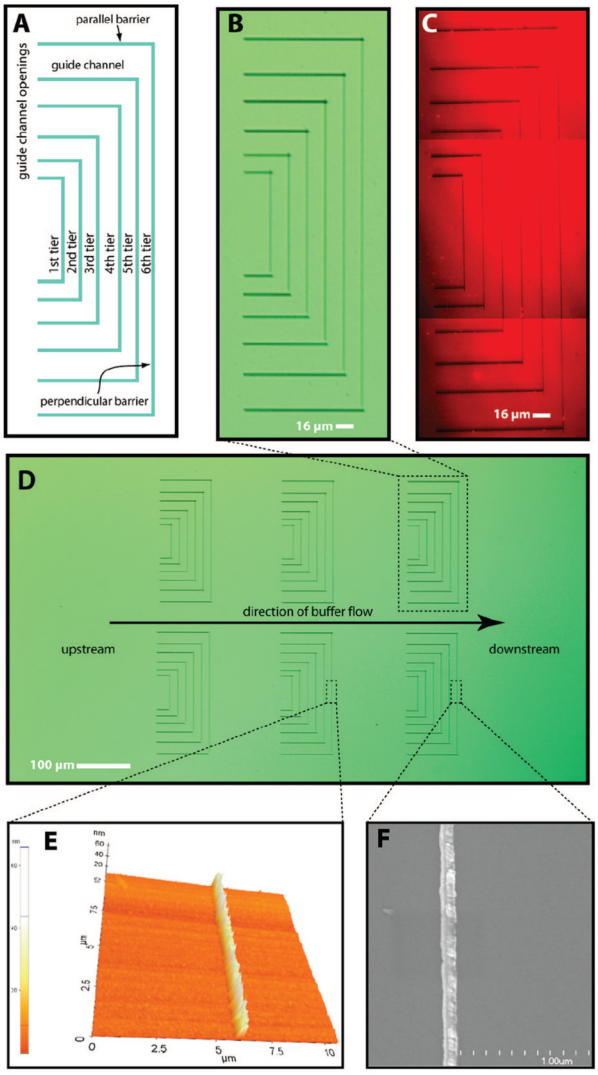

Figure 2.

Patterned chromium diffusion barriers. The overall design of the desired barrier patterns is shown in (A) and the key features of the barriers are indicated. A magnified optical image of a single barrier set is shown in (B) and a composite fluorescence image of a barrier set after deposition of a bilayer containing 0.5% rhodamine-DHPE is shown in panel (C). Panel (D) shows an optical image at 10x magnification of a 2 × 3 series of barrier sets made of chromium deposited onto fused silica. The upstream and downstream areas are indicated and the arrow shows the direction that buffer would be flowing relative to the barrier patterns. Panel (E) shows an AFM image of a 10.5 × 10.5 μm^2 area of fused silica with a 31 nm tall chromium barrier. An SEM image of a typical chromium barrier viewed from above is shown in panel (F), and bars in are divided into 100 nm increments.

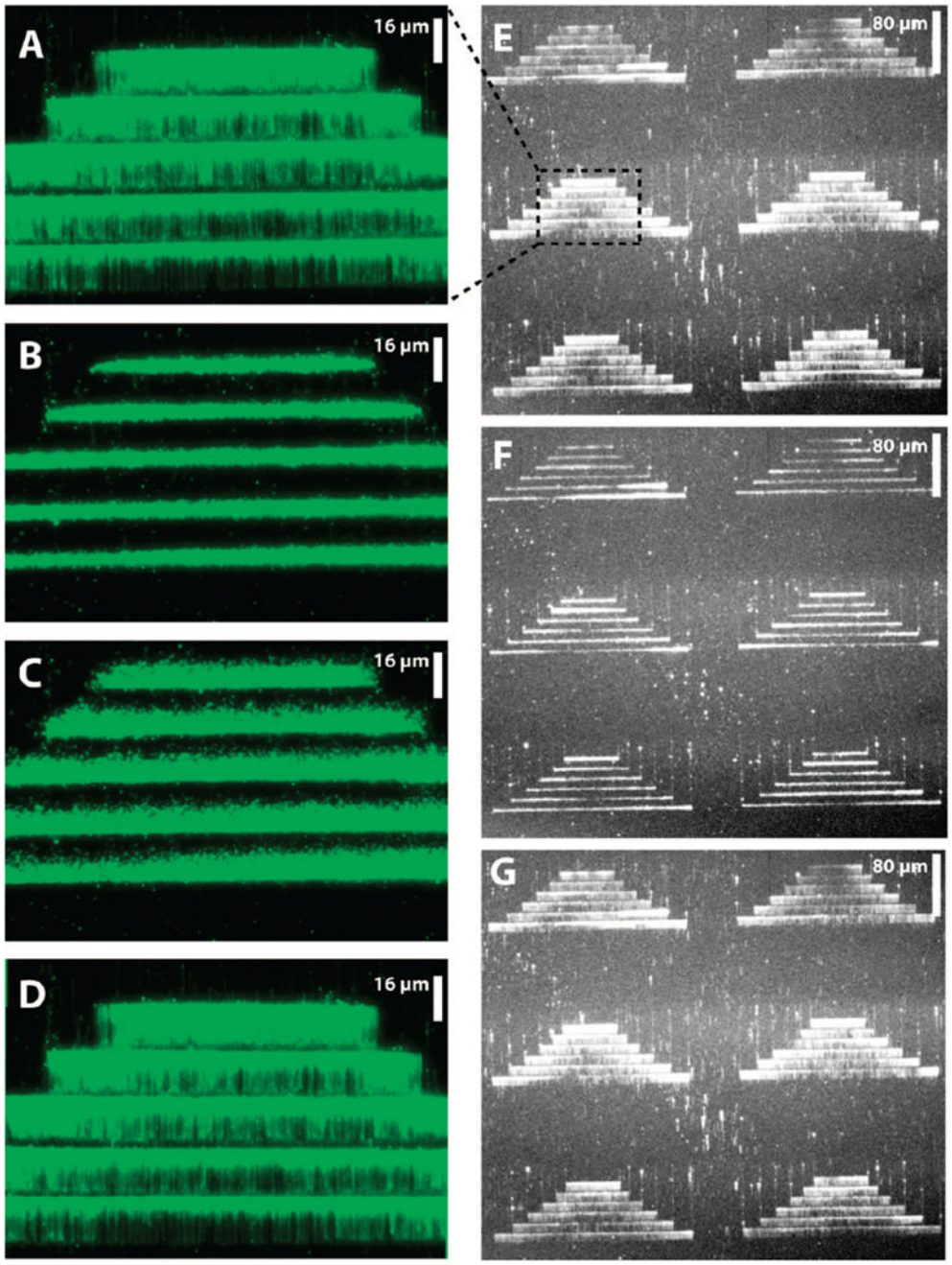

Figure 3.

Images of YOYO1-stained λ-DNA curtains assembled at the nanoscale diffusion barriers. The top panel (A) shows the DNA molecules imaged at 60× magnification after they have been aligned at the barriers. The direction of buffer flow is from top to bottom and the dashed lines are to emphasize that this image comes from a surface with multiple barrier sets. There are ~805 DNA molecules in this single image (~150, 185, 185, 155, and 130 molecules in the first, second, third, fourth, and fifth tiers, respectively). Panel (B) shows the response of the DNA molecules immediately after stopping buffer flow. This shows that the molecules rapidly retract from the surface, leaving only their tethered ends within the evanescent field. In panel (C) the DNA molecules have begun to diffuse away from the

chromium barrier and panel (D) shows the same field of view immediately after buffer flow was resumed, causing the DNA molecules to realign at the barriers. Panels (E–G) show a 2 × 3 series of barrier sets viewed at 10× magnification with buffer flow on, without buffer flow, and then after resumed flow, respectively. The uneven fluorescence signal in the 10× image is due to heterogeneity in the evanescent field.

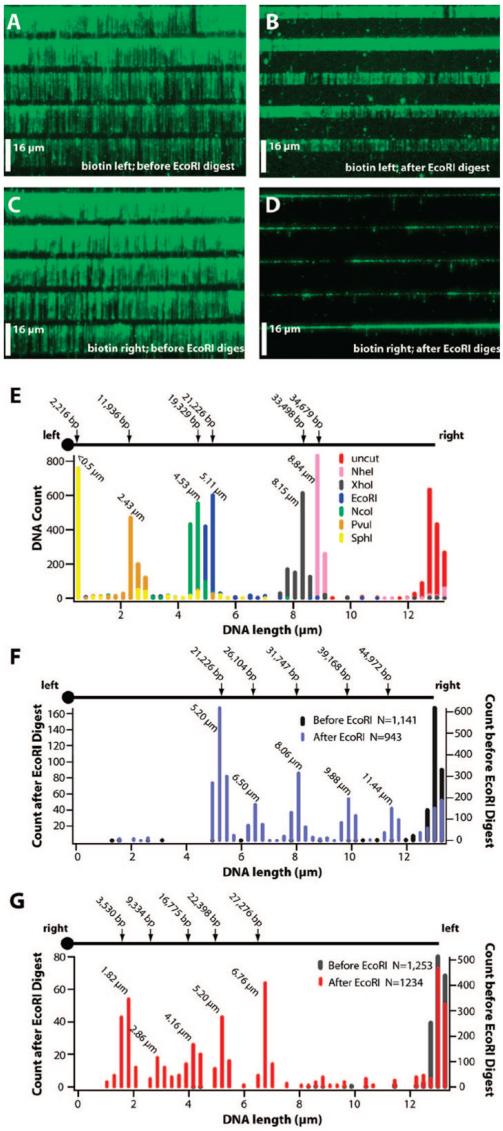

Figure 4.

Physical mapping of a λ-DNA curtain. A curtain of λ-DNA tethered by the left ends of the molecules is shown before (A) and after (B) complete digestion with *Eco*RI, which yields a ~21 kb tethered product. Panels (C) and (D) show λ-DNA tethered by the right ends before and after digestion with *Eco*RI, which is expected to yield a 3.5 kb tethered product. The images and histograms in panel (E) show the length distributions (measured from the barrier edge to the end of the DNA) of uncut λ-DNA tethered via the left end following a series of successive digests with Nhe I, Xho I, *Eco*RI, Nco I, Pvu I, and Sph I. The histograms in (F) and (G) show the results of partial *Eco*RI digests with λ-DNA tethered by either the left or right ends, respectively. Fragments outside the peak values were due to either laser induced double-stranded breaks of the YOYO1 stained DNA or uncut DNA molecules.

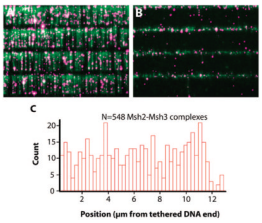

Figure 5.

Protein binding distributions measured with nanofabricated DNA curtains. Panels (A–B) show an example of fluorescently tagged Msh2-Msh3 bound to curtains of DNA, before and after transiently pausing buffer flow, respectively. The proteins are shown in magenta and the DNA molecules are in green. Panel (C) shows a kymogram of the Msh2-Msh3 binding distribution, and the positions of the proteins were measured as described.[25]